PLASMA MODELING OF WAKEFIELDS IN ELECTRON CLOUDS*

T. Katsouleas, A. Z. Ghalam, S. Lee,
University of Southern California (USC)
W. B. Mori, C. Huang, V. Decyk, C. Ren
University of California at Los Angeles (UCLA)

Abstract

To estimate the importance of collective fields of an electron cloud interacting with a positively charged particle beam, we apply two particle-in-cell codes from plasma physics – OSIRIS and QuickPIC. These codes have been used extensively to model the wakefields excited by positron bunches in a neutral plasma in the scheme known as the plasma wakefield accelerator (PWFA). The collective wakefields excited in the electron cloud plasma are similar. Analytic estimates and numerical solutions for the wakefields are obtained and their importance assessed. The basic approach as well as special features of the codes such as moving windows and quasi-static wakefield approximations are described.

1 INTRODUCTION

The need to understand the interaction of intense positively charged beams with the low density electron clouds they create in circular accelerators is well documented. These low density clouds constitute a non-neutral plasma which supports wakefields of the beam. The wakefields affect the beam propagation in a number of ways. They lead to focusing terms that alter the tune shift of the accelerator, longitudinal terms affecting the synchrotron motion and deflection terms that couple small offsets between the head and tail. The latter are believed to be responsible for a head–tail instability that leads to emittance blow-up and limits the beam current in many existing and planned circular accelerators.

Several simulation models have been developed for the wakes and instability of beams in electron clouds. These typically have many approximations such as neglect of the space charge of the cloud on itself, and condensation of the effect of the cloud to a single kick on the beam once per turn. Perhaps of even greater concern is the newness of the models themselves. As a result there has been little opportunity to benchmark the codes against reference codes or experimental data.

In this paper we apply some of the simulation tools we have been developing over the past decade for the study of plasma-based accelerators to the problem of wake production and beam propagation in electron clouds. Particularly relevant are recent benchmarks of these tools against a beam-driven plasma wakefield experiment at SLAC known as E-162. In that experiment, positron beams are propagated through a 1.4 meter long plasma. The physical mechanism of wakefield production; namely, the rapid drawing in of plasma electrons to the beam axis on a beam plasma frequency time-scale is nearly identical in this experiment and in the case of electron clouds in circular machines. In the remainder of this paper, we briefly review two primary simulation models we use, OSIRIS and QuickPIC, along with sample benchmarks of these codes. Then we apply them to the case of electron cloud wakefields in the SPS proton storage ring at CERN. Comparisons are made to recent models by Rumolo and Zimmerman [1]. We also examine the propagation of tilted and untilted beams through a significant length of the accelerator (40 km) in their self-consistent wakefields. The effects of the cloud wake and image forces from the wall are isolated and discussed. Finally, we comment on prospects for creating a complete high-fidelity PIC model that includes all of the relevant plasma physics contained here as well as the lattice terms and synchrotron motion of other models. Through high performance computing it may be possible to use such a model to make accurate predictions over thousands of turns. We compare analytic expressions for cloud wakefield amplitudes that we have obtained [2] and compare them to the simulations.

2 DESCRIPTION OF SIMULATION MODELS - OSIRIS AND QUICKPIC

Our primary simulation tools for beam–plasma interactions are the particle-in-cell (PIC) codes OSIRIS [3] and QuickPIC [4]. We describe each briefly here. OSIRIS is a fully self-consistent, fully relativistic, fully electromagnetic 3-D plasma PIC code. It solves Maxwell's equations on a 3-D Cartesian grid by finite difference in the time domain. The current and charge density sources for Maxwell's equations are found by depositing the positions and velocities of a collection of 10^6–10^8 charged particles on the grid. The fields are then used to update the particles' positions and velocities and the cycle is repeated. The code features a moving window (to follow a beam), is object-oriented and parallel. We have used this code to model the E-162 experiments at full scale in 3-D. This typically requires 1–10 GBytes of memory and 10^3 or more CPU hours. Such codes have proved to be highly reliable, but are obviously computationally intensive.

QuickPIC is a 3-D PIC code using a quasi-static or frozen field approximation [5]. This approximation is specifically useful for studying wakes. It requires that the beam not evolve significantly on the time scale that it takes the plasma to pass through it, or in other words, $\beta \gg \sigma_z$.

* Work supported by USDoE

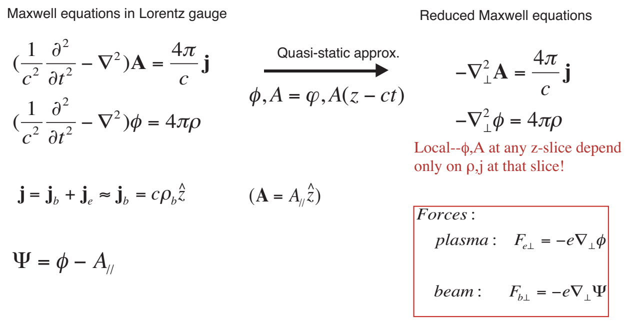

Figure 1: Quasi-static or frozen field approximation used in QuickPIC

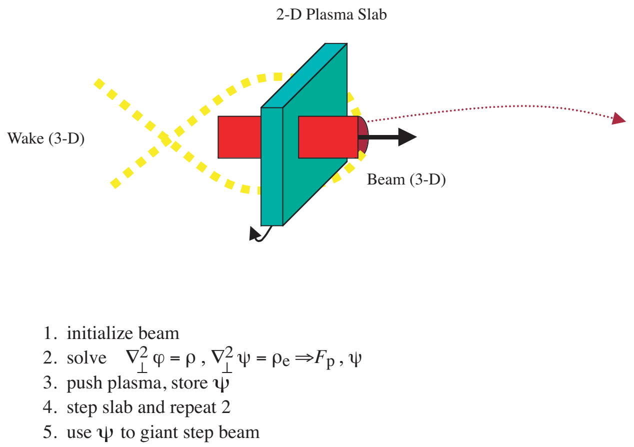

Figure 2: QuickPIC cycle. It uses a 2-D Poisson solver to calculate potentials and update particles

This is typically well satisfied. The basic equations for QuickPIC follow from the wave equations for A and ϕ in the Lorentz gauge [5] as illustrated in the box in Fig. 1.

The quasi-static approximation assumes that the wakes are functions of $z -$ ct only and leads to equations for the wake potentials φ and $\Psi = \varphi - A_{||}$ that involve only solving 2-D Poisson equations. The QuickPIC cycle is illustrated in Fig. 2. The Poisson equations are solved on a 2-D slab of plasma (using a well-established bounded 2-D PIC code BEPS as a subroutine) with conducting boundary conditions.

The wakes are stored and used to update the plasma in the slab and the slab is then pushed back a small step through the beam. After transiting the beam, the stored values of φ are used to find the force on the beam (treated as a 3-D PIC model) and it is pushed through a large step (of the order β/30). The need to solve for only a 2-D slab and the larger time steps of the 3-D push enable a time saving of 2–3 orders of magnitude. Both the 3-D outer layer and the 2-D inner layer of the code have been written in a parallel fashion to allow domain decomposition along z and y, respectively.

A comparison of QuickPIC and OSIRIS output for E-157 is shown in Fig. 3. In this experiment the wake

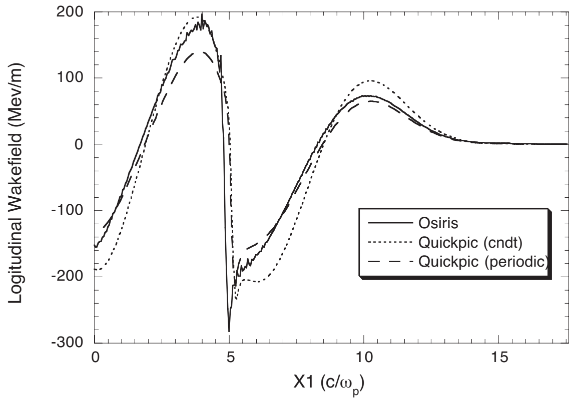

Figure 3: Wakefields for the E-157 experiment with OSIRIS and QuickPIC

Table 1: Parameters of SPS and KEKB

Variable	Symbol	SPS	KEKB
Bunch population $[10^{10}]$	N_b	10	3.3
Beam momentum [GeV/c]	p	26	3.5
Circumference [km]	C	6.9	3.0
Electron density $[10^{12}$ m$^3]$	e	1	1
rms bunch length [mm]	z	300	4
rms hor. beam size [mm]	x	3	0.4
rms vert. beam size [mm]	x	2.3	0.06

is produced by a Gaussian bunch of electrons of density 10^{15}/cm^{-3} and bunch length $\sigma_z = 0.63$ mm in a plasma of density 2×10^{14}/cm^{-3}. The agreement between the two models is reasonably good in this case. The basic QuickPIC algorithm reproduces the more exact model so long as the plasma motion is dominantly radial and the radial velocity is not relativistic, conditions that are typical also in the electron cloud regimes of interest here. Accordingly we will use QuickPIC in the simulations presented in the remainder of this paper.

Next we apply QuickPIC to the electron cloud case. We remove the background ions usually present in the plasma simulations and initialize a cloud and beam with the parameters used previously [1] for the SPS ring at CERN. The parameters are given in Table 1.

Figure 4 shows the initial beam and cloud density profiles in the X-Z plane. From this we see that cloud electrons are sucked in reaching a peak density enhancement factor of 150 at a location 1.9σ behind the beam.

The analytically expected enhancement factor at the center of the beam is given in Ref. [2] to be approximately 100 and in the simulation it is 70. The cloud response gives rise to the wakefields shown in Fig. 5.The longitudinal wake field reaches a maximum retarding field of 10 V/m near the center of the beam. This compares to the analytic expression in Ref. [2], which estimates the field at the center to be about 10 V/m.

Also for comparison we reproduce the results of Rumolo and Zimmermann [1] in Fig. 6. For identical parameters

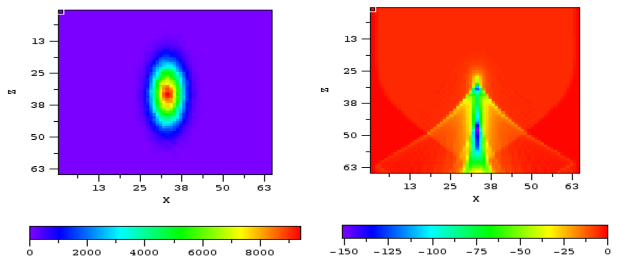

Figure 4: Initial beam and plasma density. Cloud electrons are sucked in at 1.9σ behind the beam.

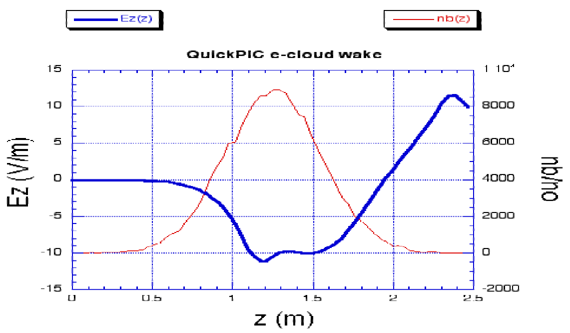

Figure 5: Longitudinal force on the beam at 1.9σ behind the beam

we see that the QuickPIC result and ECLOUD results are quite similar in the main part of the beam, but the ECLOUD result has unphysical divergences at the extreme head and tail.

In Fig. 7 we show corresponding results for the tilted beam. The beam is initially tilted by σ_r over σ_z of the bunch.

The structure of the cloud density in Fig. 7 is interesting and can be understood as follows: A compression peak is formed along the tilted axis of the beam due to the drawing in of electrons nearest the beam. Electrons from further away (nearest the pipe walls), receive their strongest kick

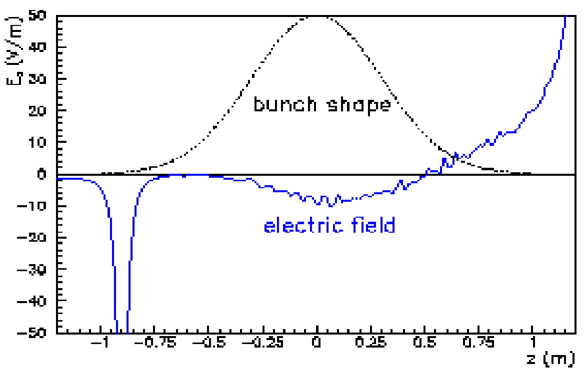

Figure 6: Longitudinal force on the beam from the electron cloud

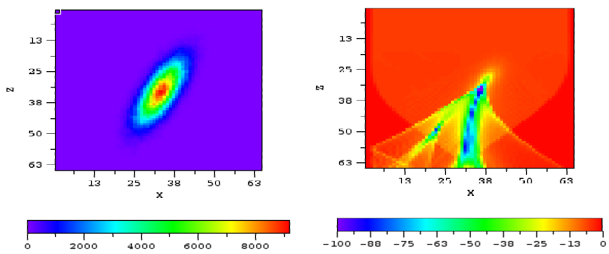

Figure 7: Initial tilted beam and plasma density. The beam is tilted σ_r over the bunch length

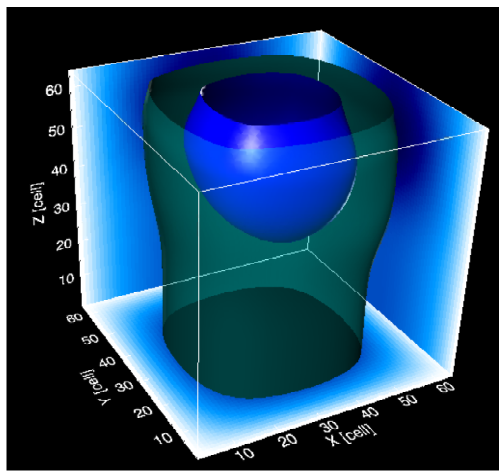

Figure 8: Wakefield potential Ψ on the beam

from the peak of the beam current (in the center of the box). By the time they arrive at the axis, they have fallen behind creating the compressions on axis at the bottom of the figure. Figure 8 shows a 3-D image of the wake potential Ψ acting on the beam. The potential at the head of the beam is attractive to the center of the pipe and is caused largely by the unperturbed cloud charge later in the beam. Later in he beam there are deflecting focusing forces coming directly from the cloud as well as from the image of the cloud in the conducting walls. We note that without the conducting boundary conditions the restoring force from the image charges would not be present.

This effect has been omitted in past work [1]. The cloud's image contributes a coherent tune shift that is larger than and in the opposite direction to the number of tune shifts caused by the image charge of the beam itself. This is because of the usual cancellation of the electric and magnetic forces between the beam and its image to order of $1/\gamma^2$. This (just as for the space charge correction to the incoherent tune shift), in the presence of the electron cloud, the tune shift due to image charges should be modified as follows:

$$\Delta\nu = A_{image} \qquad (\text{no } e_{cloud}) \tag{1}$$

$$\Delta\nu = A_{image}(1 - \eta_e\gamma^2) \qquad (\text{with } e_{cloud}) \ , \tag{2}$$

where η_e is the fractional neutralization of the beam.

$$\eta_e = H_e n_c / n_b = \eta_e(z) \ , \tag{3}$$

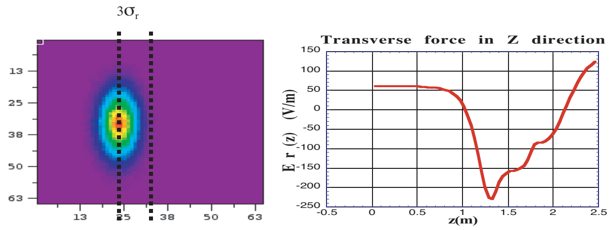

Figure 9: Right: Beam offset by $3\sigma_r$, Left: Plots of $\partial\Psi/\partial x$ at $x = 3\sigma_r$

where n_c is the cloud density before the beam and n_b is the beam density.

Note that $\Delta\nu$ varies along the bunch providing an additional mechanism for head–tail offsets to form and/or grow. Figure 9 shows simulation results for an offset beam. We next study the beam evolution in the wake potentials above. In these simulations, there is no external field (i.e., no lattice), and the emittance is artificially low thus they should be taken as cartoons to illustrate (and in some sense isolate) just the wakefield effects on propagation. Further work is needed to include the external environment of the storage ring. In these simulations the 3-D time step is 50 m. Figure 10 shows snapshots of the beam and cloud at propagation distance of $z = 0, 5, 10, 15$ and 20 km. We see the dynamic focusing of the beam by the cloud. At later times a small tail oscillations in the beam and cloud density is seen in the movies. This oscillation grows despite the fact that the beam and cloud are initially symmetric except for small numerical noise. The instability does not continue to grow in this example and saturates after 20 km of propagation. Figure 11 shows the corresponding evolution of an initially tilted beam. The tail oscillation is much more pronounced in this case.

In summary, we have applied simulation tools developed and benchmarked for plasma-based accelerator research to the problem of beam propagation in circular accelerators with low density electron clouds present. We find the wakefields compare well with analytic estimates and previous models over most conditions. We also find a new contribution to the coherent tune shift of the accelerator due to electron cloud image forces not included in previous models. We believe the combining of our quasi-static PIC models (QuickPIC) with the relevant lattice of circular accelerator models could lead to a powerful tool for predicting the onset and evolution of electron cloud instabilities. It appears that the capability for massively parallel computation with QuickPIC would enable modeling with PIC accuracy to be extended to relevant lengths (i.e., several thousand turns).

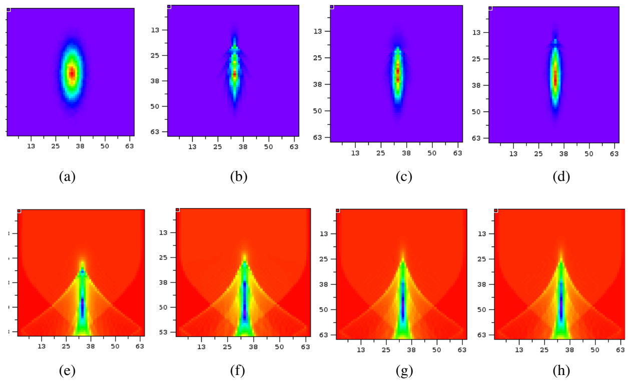

Figure 10: Snapshots of Beam (a-d) and cloud (e-h) density

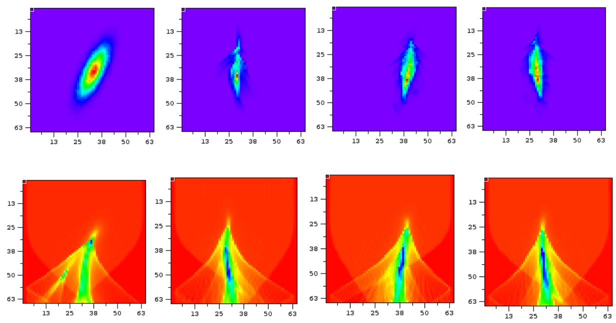

Figure 11: Corresponding Snapshots with tilted beam

3 ACKNOWLEDGEMENTS

We would like to thank Frank Zimmermann for introducing us to this problem and G. Rumolo, F. Decker, Wei Jei, C. Clayton, Bob Siemann, and the E-162 Collaboration for useful discussions. Work supported by DOE and NSF.

4 REFERENCES

[1] G. Rumolo and F. Zimmermann, Longitudinal Wake due to Electron Cloud.

[2] A.Z. Ghalam et al., in preparation.

[3] R. Hemker et al., Proc. 1999 Part. Accel. Conf. (1999).

[4] C. Choung et al., in preparation.

[5] D.H. Whittum, Phys. Plasmas, vol. 4, p. 1154, 1997.